1999년도 한국음향학회 학술발표대회 논문집 제18권 제2(s)호

압전체 시뮬레이션을 위한 전극 방향 변환 고려

장순석*, 안흥구**, 이제형**, 최현호***
조선대학교 전기.제어계측공학부*, 조선대학교 대학원 제어계측공학과**, 조선대학교 제어계측공학과***

Consideration of Poling Direction Transformation for Piezoelectric Simulation

Soon Suck Jarng, Heung Gu Ahn, Je Hyeong Lee, Heun Ho Choi
Dept. of Electrical Control & Instrumentation, Chosun University

1. Introduction

Electrostrictive (or piezoelectric) materials such as lead zirconate titanate (PZT) and barium titanate ($BaTiO_3$) are used as main parts of an electroacoustic sensor. Sonar transducer is an example of the electroacoustic sensor. The performance of any electroacoustic sensor could be improved either by using a new sophisticated electrostrictive material or by better structural design. Especially the frequency response and the directivity pattern of the electroacoustic sensor very much depend on the type and dimension of the electrostrictive material and any adjacent elastic composite material. Therefore much research works have been carried out in respect of the structural design of the electroacoustic sensor. As the structure of the electroacoustic sensor necessarily becomes complicated due to higher functional performance, numerical analysis is more preferred than analytical solution. The finite element method (FEM) is perhaps the most suitable method for the structural simulation of the electrostrictive material. Also the boundary element method (BEM) is readily coupled with the FEM by which the acoustic field problem of the electroacoustic sensor can be solved directly. The piezoelectricity of the electrostrictive material is mathematically expressed by the pair of piezoelectric equations in tensor form;

$$T_{ij} = C^{E}_{ijkl} S_{kl} - e_{ijn} E_n$$
$$q_m = e_{mkl} S_{kl} + \varepsilon^{S}_{mn} E_n \qquad (1)$$

The index notation is based on cartesian co-ordinates. Also equation (1) can be expressed in matrix form

$$[T] = [C^{E}][S] - [e]\varepsilon^{S}[E] \qquad (2)$$
$$[q] = [e]^{t}[S] + [][E]$$

And equation (3) shows the details of the matrix components of equation (2).

The stiffness coefficient matrix of equation (3) is a general three dimensional matrix form for any isotropic, orthotropic and anisotropic material property. It should be noticed that most of stiffness coefficient matrix, [C], are measured with respect of Z-axis reference/poling direction. In modelling of the dynamic mechanism of orthotropic electrostrictive materials, the local co-ordinates of the poling direction should be clarified. It is very difficult to find any reference about the transformation of the local co-ordinates for a polarized electrostrictive material in any direction. This paper clearly explains about this problem with FEM examples.

2. Finite element-boundary element modelling

2.1 Piezoelectric matrix equations

Modelling of a electrostrictive transducer in this paper is based on a virtual work principle [1]. The active electrostrictive material PZT4 is polarized with two electrodes. The dynamics of the piezoelectricity is assumed to be linear in modelling. The set of constitutive laws which govern the electrostrictive transduction process can be modelled three-dimensionally by the pair of piezoelectric equations applied to a single point in the bounded electrostrictive continua in tensor form as shown in equation (1). The principle of the FEM is that the variables in the piezoelectric equations at a point within an element is approximated throughout the element by interpolation between nodal values;

$$[u] \cong [N_u][a] \quad \text{and} \quad u_\phi \cong [N_\phi][\phi] \qquad (4)$$

where $[u]$ is a 3x1 displacement vector, $[a]$ is a 60x1 nodal displacement vector, u_ϕ is an electric potential scalar, $[\phi]$ is a 20x1 nodal electric potential vector. $[N_u]$ and $[N_\phi]$ are interpolation (shape) functions with respect of displacement and electric potential nodal vectors respectively.The elasticity of the electrostrictive material obeys the Newton's law while the electricity of the electric field obeys the Poisson's law.

Newton's law $[S] = [D_u][u]$ (5a)

Poisson's law $[E] = -[D_\phi]u_\phi$ (5b)

When equation (4) is applied to equation (5);

$$[S]=[D_u][u] \cong [D_u][N_u][a] \equiv [D_S][a] \quad (6a)$$

$$[E]=-[D_\phi]u_\phi \cong -[D_\phi][N_\phi][\phi] \equiv -[D_E][\phi] \quad (6b)$$

The piezoelectric equations are partial differential equations and their solution is therefore derived as an integral matrix formulation with boundary conditions. Since the basis of FEM is a direct integration process at the level of finitely discretized elements, the piezoelectric equations are transformed to an integral form by means of various techniques such as the virtual work method, the variational method and the weighted residual method [1]. When some external energy such as mechanical force and/or electrical current is imposed on the electrostrictive transducer, the applied energy is absorbed throughout the transducer and is transformed into another form. This relationship can be expressed in an elemental matrix form as only one element is considered according to the virtual work principle [2]:

$$[\delta a]^t[F]=\int_V[\delta S]^t[T]dV+\int_V[\delta u]^t\rho[\ddot{u}]dV \quad (7a)$$

$$[\delta\phi]^t[Q] = \int_V[\delta E]^t[q]dV \quad (7b)$$

where [F] is an external force vector and [Q] is an applied charge vector on elemental nodes and ρ is the density of the material. If equation (2) and equation (6) are applied to equation (7a),

$$\begin{aligned}[\delta a]^t[F] &= \int_V[\delta S]^t[T]dV+\int_V[\delta u]^t\rho[\ddot{u}]dV \\ &\cong \int_V[\delta S]^t[C][S]dV-\int_V[\delta S]^t[e][E]dV+ \\ &\quad \int_V[\delta a]^t[N_u]^t\rho[N_u][\ddot{a}]dV \\ &\cong \int_V[\delta a]^t[D_S]^t[C][D_S][a]dV-\int_V[\delta a]^t[D_S]^t \\ &\quad [e][E]dV-\omega^2\int_V[\delta a]^t[N_u]^t\rho[N_u][a]dV \\ &\cong \int_V[\delta a]^t[D_S]^t[C][D_S][a]dV+\int_V[\delta a]^t[D_S]^t \\ &\quad [e][D_E][\phi]dV-\omega^2\int_V[\delta a]^t[N_u]^t\rho[N_u][a]dV\end{aligned} \quad (8)$$

Equation (8) is re-written without $[\delta a]^t$ as follows

$$[F] \cong \int_V[D_S]^t[C][D_S]dV[a]+\int_V[D_S]^t[e][D_E]dV[\phi] -\omega^2\int_V[N_u]^t\rho[N_u]dV[a] \quad (9)$$

Also when equation (2) and equation (6) are applied to equation (7b),

$$\begin{aligned}[\delta\phi]^t[Q] &= \int_V[\delta E]^t[q]dV \\ &\cong \int_V-[\delta\phi]^t[D_E]^t[q]dV \\ &\cong \int_V-[\delta\phi]^t[D_E]^t[e]^t[S]dV+ \\ &\quad \int_V-[\delta\phi]^t[D_E]^t[\varepsilon][E]dV \\ &\cong \int_V-[\delta\phi]^t[D_E]^t[e]^t[D_S][a]dV+ \\ &\quad \int_V[\delta\phi]^t[D_E]^t[\varepsilon][D_E][\phi]dV\end{aligned} \quad (10)$$

The last expression of equation (10) is re-written without $[\delta\phi]^t$:

$$-[Q] \cong \int_V[D_E]^t[e]^t[D_S]dV[a]+\int_V-[D_E]^t[\varepsilon][D_E]dV[\phi] \quad (11)$$

The pairs of equation (9) and equation (11) are defined as piezoelectric matrix equations and is given as short form as follows.

$$[F] = [K_{uu}][a]-\omega^2[M][a]+[K_{u\phi}][\Phi]$$
$$-[Q] = [K_{\phi u}][a]+[K_{\phi\phi}][\Phi] \quad (12)$$

The volume integration of the piezoelectric matrix equations is done in local coordinates by three-dimensional Gauss-qadrature formula [2]:

$$[K_{uu}]=\int_{-1}^{+1}\int_{-1}^{+1}\int_{-1}^{+1}[D_S]^t[C^E][D_S]|Ja|d\xi d\eta d\zeta$$

$$[K_{u\phi}]=\int_{-1}^{+1}\int_{-1}^{+1}\int_{-1}^{+1}[D_S]^t[e][D_E]|Ja|d\xi d\eta d\zeta$$

$$[K_{\phi u}]=\int_{-1}^{+1}\int_{-1}^{+1}\int_{-1}^{+1}[D_E]^t[e]^t[D_S]|Ja|d\xi d\eta d\zeta$$

$$[K_{\phi\phi}]=-\int_{-1}^{+1}\int_{-1}^{+1}\int_{-1}^{+1}[D_E]^t[\varepsilon^S][D_E]|Ja|d\xi d\eta d\zeta$$

$$[M]=\int_{-1}^{+1}\int_{-1}^{+1}\int_{-1}^{+1}[N_u]^t\rho[N_u]|Ja|d\xi d\eta d\zeta \quad (13)$$

where ξ, η, ζ are local cartesian coordinates and Jacobian matrix [Ja] is derived as

$$[Ja] = \begin{bmatrix} \frac{\partial N^1}{\partial\xi} & \frac{\partial N^2}{\partial\xi} & \cdots & \frac{\partial N^n}{\partial\xi} \\ \frac{\partial N^1}{\partial\eta} & \frac{\partial N^2}{\partial\eta} & \cdots & \frac{\partial N^n}{\partial\eta} \\ \frac{\partial N^1}{\partial\zeta} & \frac{\partial N^2}{\partial\zeta} & \cdots & \frac{\partial N^n}{\partial\zeta} \end{bmatrix} \cdot \begin{bmatrix} x^1 & y^1 & z^1 \\ x^2 & y^2 & z^2 \\ \cdots & & \\ \cdots & & \\ \cdots & & \\ x^n & y^n & z^n \end{bmatrix} \quad (14)$$

where n=20 for each element and N is a quadratic three-dimensional isoparametric shape function.

2.2 Transformation of local co-ordinates for differnet poling directions

Two different types of local co-ordinates' transformation should be considered when the polarizing direction is concerned. One is due to the physical change of the poling direction from Z-axis to any direction in 3 dimensional axes. The other is related with geometric rotation. Fig. 2 shows a typical variation of the poling direction such as from Z-axis to radial axis.

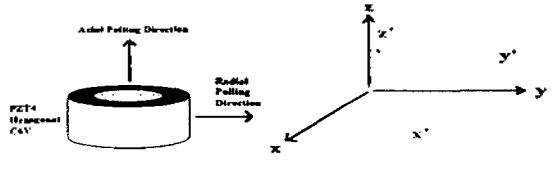

(a) (b)

Fig. 2 (a) Change of poling direction from Z-axis to radial axis, (b) Changed local co-ordinates (x',y',z') from initial global cartesian co-ordinates (x,y,z)

Fig. 2 (b) shows the changed local co-ordinates (x', y', z') from the initial global cartesian co-ordinates (x, y, z). In figure 2 (b) Z'-axis indicates the new poling direction rotated from the original Z-axis. According to the tensor theory applied to the pair of piezoelectric equations, the coefficient matrices must be

changed when the poling direction is varied.

$$T'_{kl} = C^E_{klij}\frac{\partial x'_k}{\partial x_k}\frac{\partial x'_l}{\partial x_l}\frac{\partial x_i}{\partial x'_i}\frac{\partial x_j}{\partial x'_j} S_{ij} - e_{klm}\frac{\partial x'_k}{\partial x_k}\frac{\partial x'_l}{\partial x_l}\frac{\partial x_m}{\partial x'_m} E_m \quad (16a)$$

$$q_n = e_{nij}\frac{\partial x_n}{\partial x'_n}\frac{\partial x_i}{\partial x'_i}\frac{\partial x_j}{\partial x'_j} S_{ij} + \varepsilon^S_{nm}\frac{\partial x_n}{\partial x'_n}\frac{\partial x_m}{\partial x'_m} E_m \quad (16b)$$

where the primed variables represent newly transformed variables in poling direction. $\frac{\partial x'_k}{\partial x_i}$ is defined as $\cos(\theta_{k,i})$ in which $\theta_{k,i}$ is the angle in radian between the x'_k axis and the x_i axis.

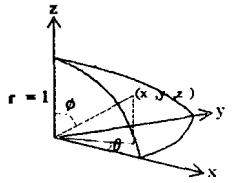

Fig. 3 A point (x,y,z) indicating a new poling direction and its angle (ϕ , θ)

In order to calculate tramsformed coefficient matrices according to the poling direction by amount of (ϕ, θ) as shown in figure 4, two matrices, $[M_1]$ and $[M_2]$, are firstly calculated.

$$[M_1] = \begin{bmatrix} \cos(\phi)\cos(\theta) & \cos(\phi)\sin(\theta) & -\sin(\phi) \\ -\sin(\theta) & \cos(\theta) & 0 \\ \sin(\phi)\cos(\theta) & \sin(\phi)\sin(\theta) & \cos(\phi) \end{bmatrix} \equiv \begin{bmatrix} a_{11} & a_{12} & a_{13} \\ a_{21} & a_{22} & a_{23} \\ a_{31} & a_{32} & a_{33} \end{bmatrix} \quad (17)$$

$$[M_2] = \begin{bmatrix} \frac{a_{11}}{\sqrt{a_{11}^2+a_{12}^2+a_{13}^2}} & \frac{a_{12}}{\sqrt{a_{11}^2+a_{12}^2+a_{13}^2}} & \frac{a_{13}}{\sqrt{a_{11}^2+a_{12}^2+a_{13}^2}} \\ \frac{a_{21}}{\sqrt{a_{21}^2+a_{22}^2+a_{23}^2}} & \frac{a_{22}}{\sqrt{a_{21}^2+a_{22}^2+a_{23}^2}} & \frac{a_{23}}{\sqrt{a_{21}^2+a_{22}^2+a_{23}^2}} \\ \frac{a_{31}}{\sqrt{a_{31}^2+a_{32}^2+a_{33}^2}} & \frac{a_{32}}{\sqrt{a_{31}^2+a_{32}^2+a_{33}^2}} & \frac{a_{33}}{\sqrt{a_{31}^2+a_{32}^2+a_{33}^2}} \end{bmatrix} \quad (18)$$

$[M_1]$ matrix is 3x3 $\theta_{k,i}$ of equation (16) for each different k and i and $[M_2]$ matrix is 3x3 $\cos(\theta_{k,i})$. Then transformed coefficient matrices of equation (16) are calculated as follows;

$$C'(i,j) = C^E_{klij}\frac{\partial x'_k}{\partial x_k}\frac{\partial x'_l}{\partial x_l}\frac{\partial x_i}{\partial x'_i}\frac{\partial x_j}{\partial x'_j} = \sum_{k=1}^{3}\sum_{l=1}^{3}\sum_{m=1}^{3}\sum_{n=1}^{3} M_2(i_1,k)M_2(i_2,l) M_2(j_1,m)M_2(j_2,n)C^E(g(k,l),g(m,n))$$

$$(1\le i\le 6\ ,\ 1\le j\le 6) \quad (19)$$

$$e'(i,j) = e_{klm}\frac{\partial x'_k}{\partial x_k}\frac{\partial x'_l}{\partial x_l}\frac{\partial x_m}{\partial x'_m} = \sum_{k=1}^{3}\sum_{l=1}^{3}\sum_{m=1}^{3} M_2(i_1,k)M_2(i_2,l) M_2(j,m)e(g(k,l),m)$$

$$(1\le i\le 6\ ,\ 1\le j\le 3) \quad (20)$$

$$\varepsilon'(i,j) = \varepsilon^S_{nm}\frac{\partial x_n}{\partial x'_n}\frac{\partial x_m}{\partial x'_m} = \sum_{k=1}^{3}\sum_{l=1}^{3} M_2(i,k)M_2(j,l)\varepsilon^S(k,l)$$

$$(1\le i\le 3\ ,\ 1\le j\le 3) \quad (21)$$

Examples are shown below. Table 1 shows the contents of the coefficient matrices of equation (3). The properties are a standard PZT4 material with Z-axis poling. Table 2 and Table 3 show the contents of the coefficient matrices for X-axis and Y-axis poling directions respectively. Also Table 4 and Table 5 show those for XY-axis (1,1,0) and XYZ-axis (1,1,1) poling directions respectively.

Table 1 Standard material properties of PZT4 with Z-axis poling.

13.9E+10	7.78E+10	7.43E+10	0	0	0
7.78E+10	13.9E+10	7.43E+10	0	0	0
7.43E+10	7.43E+10	11.5E+10	0	0	0
0	0	0	2.56E+10	0	0
0	0	0	0	2.56E+10	0
0	0	0	0	0	3.06E+10
0	0	0	0	12.7	0
0	0	0	12.7	0	0
-5.2	-5.2	15.1	0	0	0
0.648E-8	0	0			
0	0.648E-8	0			
0	0	0.562E-8			

Table 2 Transformed material properties of PZT4 with X-axis poling.

11.5E+10	7.43E+10	7.43E+10	0	0	0
7.43E+10	13.9E+10	7.78E+10	0	0	0
7.43E+10	7.78E+10	13.9E+10	0	0	0
0	0	0	3.06E+10	0	0
0	0	0	0	2.56E+10	0
0	0	0	0	0	2.56E+10
-15.1	5.2	5.2	0	0	0
0	0	0	0	0	-12.7
0	0	0	0	-12.7	0
0.562E-8	0	0			
0	0.646E-8	0			
0	0	0.646E-8			

Table 3 Transformed material properties of PZT4 with Y-axis poling.

13.9E+10	7.43E+10	7.78E+10	0	0	0
7.43E+10	11.5E+10	7.43E+10	0	0	0
7.78E+10	7.43E+10	13.9E+10	0	0	0
0	0	0	2.56E+10	0	0
0	0	0	0	3.06E+10	0
0	0	0	0	0	2.56E+10
0	0	0	0	0	12.7
-5.2	15.1	-5.2	0	0	0
0	0	0	12.7	0	0
0.648E-8	0	0			
0	0.562E-8	0			
0	0	0.562E-8			

Table 4 Transformed material properties of PZT4 with XYZ-axis (1, 1, 1) poling.

13.0E+10	7.58E+10	7.58E+10	-8.33E+8	4.17E+9	4.17E+9
7.58E+10	13.0E+10	7.58E+10	-4.17E+9	8.33E+8	4.17E+9
7.58E+10	7.58E+10	13.0E+10	-4.17E+9	4.17E+9	8.33E+8
-8.33E+8	-4.17E+9	-4.17E+9	2.76E+10	1.33E+9	1.33E+9
4.17E+9	8.33E+8	4.17E+9	1.33E+9	2.76E+10	-1.33E+9
4.17E+9	4.17E+9	8.33E+8	1.33E+9	-1.33E+9	2.76E+10
-10.7	4.0	4.0	1	6.4	6.4
-4.0	10.7	-4.0	6.4	1	-6.4
-4Z.0	-4.0	10.7	6.4	-6.4	1
0.648E-8	0.280E-9	0.280E-9			
0.280E-9	0.618E-8	-0.28E-9			
0.280E-9	-0.28E-9	0.618E-8			

2.3 Transformation of local co-ordinates for differnet geometric rotations

Another type of local coordinates transformation is related with the geometric rotation of the poling direction. It means that the material property of PZT4 is not changed but the structure of the electrostrictive material is geometrically rotated. Then special care must be taken into account in programming. First of all, the jacobian matrix of equation (14) should be transformed like

$$[Ja]' = [Ja][M_1]' \tag{22}$$

For the present 20 nodes' quadratic element, the matrix size of $[K_{uu}]$ is 60x60 and that of $[K_{u\phi}]$ is 60x20. $[K_{uu}]$ can be subdivided into twenty 3x3 subelements for each local node, and also $[K_{u\phi}]$ can be subdivided into twenty 3x1 subelements for each local node. Then $x_{uu}(i,j)$ is defined as a 3x3 subelement of $[K_{uu}]$ and $x_{u\phi}(i,j)$ is defined as a 3x1 subelement of $[K_{u\phi}]$. Secondly, equation (13a)~(13b) should be transformed as follows

$$x_{uu}(i,j)' = \sum_{k=1}^{3}\sum_{l=1}^{3} M_2(i,k)M_2(j,l)x_{uu}(k,l), \quad (1\le i\le 3,\ 1\le j\le 3) \tag{23a}$$

$$x_{u\phi}(i)' = \sum_{k=1}^{3} M_1(i,k)'\, x_{u\phi}(k), \quad (1\le i\le 3) \tag{23b}$$

The idea of the matrix transformation for the geometric rotation is based on that the structure of the individual finite element is firstly rotated to be directed in Z-axis poling and is secondly integrated, and then thirdly the integrated piezoelectric matrices are re-rotated back to its initial global position.

2.4 Boundary Element Method (BEM)

This section is removed for the limit of the page numbers

2.5 Coupled FE-BEM

The coupled FE-BEM is composed of equation (13) and fluid loading matrices [11]. The pairs of equation (31) are defined as piezoelectric matrix equations representing flooded electrostrictive sonar transducer:

$$-[Q] = [K_{\phi u}][a] + [K_{\phi\phi}][\phi]$$
$$[F] = [K_{uu}][a] + [K_{u\phi}][\phi] - \omega^2[M][a] + [\rho_f \omega^2[L](A^{\oplus})^{-1}B^{\oplus}][a] \tag{31}$$

3. Results and Discussion

In section 2.2 the transformation of local co-ordinates for differnet poling directions was examined. In this section the transformation of local co-ordinates for differnet geometric rotations will be examined with a particular example. Fig. 5 shows two mixed blocks of iron and PZT4 materials with Z-axis poling direction (a) and with circumferential poling direction (b). Their poling directions of PZT4 are different because of geometric rotation, but both block models are the same in fact in their dimensions. Local cartesian co-ordinates (x,y,z) have to be transformed in order to fit their corresponding poling directions. Each block is composed of 8 elements (4 for iron, 4 for PZT4). Fig. 6 shows the electroding of positive and negative(ground) electrodes. One electrode is allocated with different weights of electric charges (Fig. 6 (c)), and the other electrode is in grounding condition.

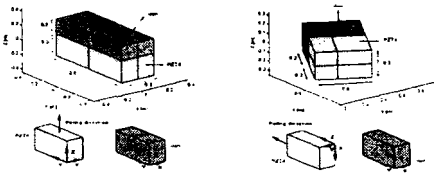

(a) (b)

Fig. 5 Mixed blocks of iron and PZT4 materials with Z-axis poling direction (a) and with circumferential poling direction (b).

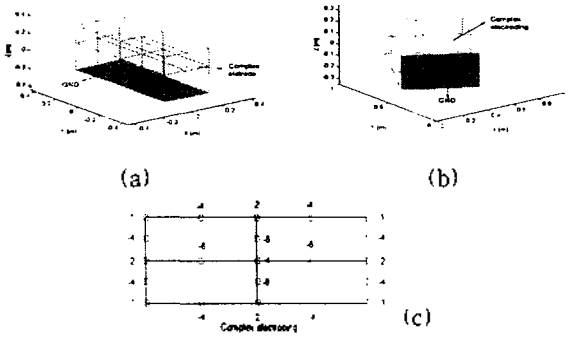

(a) (b) (c)

Fig. 6 Electrical electrodes. One electrode in different allocation of electric charges (c) and the other electrode in ground condition.

Fig. 7 shows real parts of displacement amplitudes at a mid-point of the block model (Fig. 7 (a)) and imaginary parts of displacement amplitudes at a mid-point of the block model (Fig. 7 (b)) as a function of frequency. 'x' and '◁' symbols indicate the results of the Z-axis poling block model while 'o' and '□' symbols indicate the results of the circumferential poling block model. Both results are perfectly agree each other.

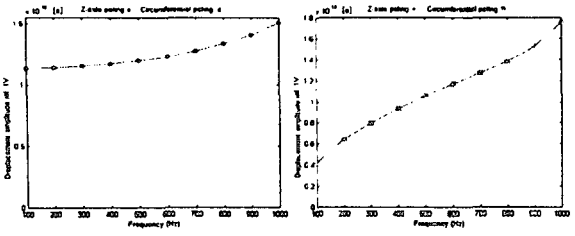

(a) (b)

Fig. 7 Real parts of displacement amplitudes at a mid-point of the block model (a) and imaginary parts of displacement amplitudes at a mid-point of the block model (b).

Fig. 8 shows real parts of electric potentials at a mid-point of the block model (Fig. 8 (a)) and imaginary parts of electric potentials at a mid-point of the block model (Fig. 8 (b)) as a function of frequency. 'x' and '+' symbols indicate the results of the Z-axis poling block model while 'o' and '□' symbols indicate the results of the circumferential poling block model. The result shows very high potential values because the model is driven by big electric charge source.

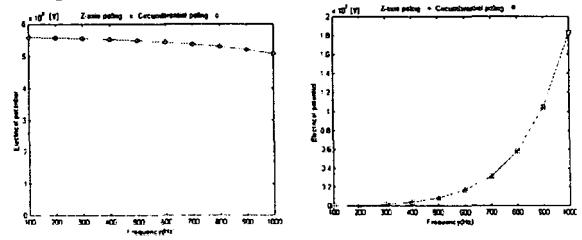

(a) (b)

Fig. 8 Real parts of electric potentials at a mid-point of the block model (a) and imaginary parts of electric potentials at a mid-point of the block model (b).

Fig. 9 shows TVRs at a far field position such as (x=0, y=0, z=100m) (Fig. 9 (a)) and TVRs at a position (x=100m, y=0, z=0) (Fig. 9 (b)). The far field positions for the circumferential poling block model, of course, are different according to its own geometric rotation.

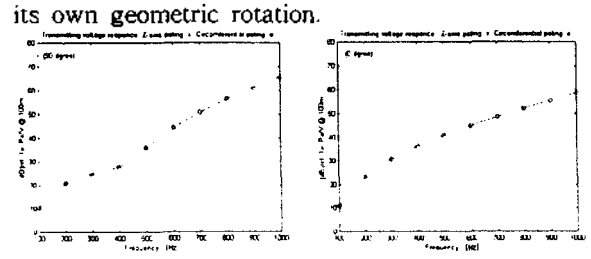

(a) (b)

Fig. 9 TVRs at a far field position (x=0, y=0, z=100m) (a) and TVRs at a position (x=100m, y=0, z=0) (b).

Fig. 10 shows the beam pattern of the block model at 1000 Hz (Fig. 10(a)) and its 3-dimensional figure (Fig. 10(b)). The scale is in dB. Finally, Fig. 11 shows the radiation impedance response of the block model sonar transducer in water. The figure is shown only between 100 Hz and 1000 Hz.

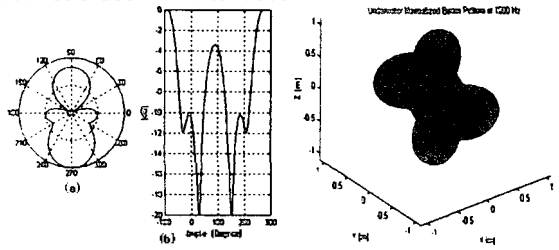

(a) (b)

Fig. 10 Beam pattern of the block model at 1000 Hz (a) and its 3-dimensional form (b).

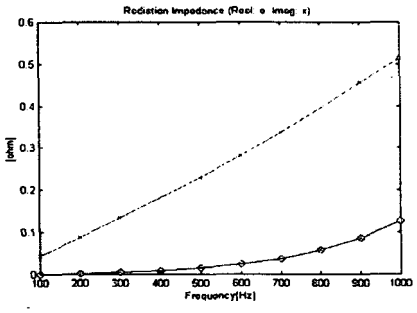

Fig. 11 The radiation impedance response of the block model sonar transducer in water.

4. Conclusion

The dynamics of the electrostrictive material, PZT4, was simulated by the coupled FE-BE method. Two different types of local co-ordinates' transformation was considered when the polarizing direction was concerned. One is due to the physical change of the poling direction from Z-axis to any direction in 3 dimensional axes. The other is related with geometric rotation. Both of local co-ordinates' transformation were examined with theoretical derivation and comparative example results.

ACKNOWLEDGMENTS

This study was supported by a grant from STEPI (Science and Technology Policy Institute) Korea, as part of the 1998 international programme of collaboration between Korea and the United Kingdom.

References

[1] Zienkiewicz O.C., "The finite element method", 3rd edition, McGraw-Hill, London, PP:178-210, 1977.

[2] Jarng S.S., "SONAR transducer analysis and optimization using the finite element method", Ph.D. Thesis University of Birmingham, 1991.

[3] L.G. Copley, "Integral equation method for radiation from vibrating bodies", J. Acoust. Soc. Am. Vol. 41, PP:807-816, 1967.

[4] L.G. Copley, "Fundamental results concerning integral representations in acoustic radiation", J. Acoust. Soc. Am. Vol. 44, PP:28-32, 1968.
[5] E. Skudrzyk, "The foundation of acoustics", (Springer-Verlag, New York, 1971), PP:408-409, Equation(76), 1971.
[6] D.T.I. Francis, "A boundary element method for the analysis of the acoustic field in three dimensional fluid-structure interaction problems", Proc. Inst. of Acoust., Vol. 12, Part 4, PP:76-84, 1990.
[7] H.A. Schenck, "Improved integral formulation for acoustic radiation problems", J. Acoust. Soc. Am. Vol. 44, PP:41-58, 1968.
[8] A.J. Burton and G.F. Miller, "The application of integral integration methods to the numerical solutions of some exterior boundary problems", Proc. R. Soc. London, Ser. A 323, PP:201-210, 1971.
[9] R.F. Kleinman and G.F. Roach, "Boundary integral equations for the three dimensional Helmholtz equation", SIAM Rev., Vol. 16, PP:214-236, 1974.
[10] D.T.I. Francis, "A gradient formulation of the Helmholtz integral equation for acoustic radiation and scattering", J. Acoust. Soc. Am. Vol. 93(4) Part 1, PP:1700-1709, 1993.
[11] S.S.Jarng, "PZT5 spherical hydrophone simulation using a coupled FE-BE method", J. of the Korean Sensors Society, Vol. 7, No. 6, pp:377-385, 1998.